XANES studies of the reduction behavior of $(Ce_{1-y}Zr_y)O_2$ and $Rh/(Ce_{1-y}Zr_y)O_2$

S.H. Overbury [a], D.R. Huntley [a], D.R. Mullins [a] and G.N. Glavee [b]

[a] *Chemical and Analytical Sciences Division, Oak Ridge National Laboratory, Oak Ridge, TN 37831-6201, USA*
[b] *Chemistry Department, Lawrence University, Appleton, WI 54912, USA*

Received 10 December 1997; accepted 25 February 1998

Using X-ray absorption near-edge spectroscopy (XANES) at the Ce L_{III} edge, we have measured the extent of reduction of Rh-loaded and Rh-free, mixed Ce–Zr oxides under hydrogen as a function of temperature. The high surface area, mixed oxides were synthesized by sol–gel techniques and hypercritical drying. Using a simple spectrum subtraction method, the degree of reduction has been measured and compared with previous results for CeO_2 and $(Ce_{0.5}Zr_{0.5})O_2$. Addition of Zr lowers the temperature of reduction and increases the extent of Ce reduction. Rh catalyzes the reduction process at low temperatures but does not substantially affect the extent of reduction achieved at high temperature. A synergism between Rh and Zr is found which leads to very high reducibility in the range of 400–600 K.

Keywords: $(Ce_{1-y}Zr_y)O_2$, CeO_2, ceria, zirconia, rhodium, Rh, X-ray absorption, XANES, metal–support interactions, temperature-programmed reduction

1. Introduction

It is widely reported that cerium oxide, a component in three-way conversion catalysts, serves to enhance the efficiency for CO conversion during rich excursions in the air/fuel ratio. The enhancement has been primarily ascribed to the oxygen exchange capability of cerium oxide which can tolerate a wide range of oxygen deficiency [1,2]. More recently, it has been reported that addition of promoters to the ceria, especially ZrO_2, can enhance the oxygen storage capacity of the ceria [3] and enhance the removal activity for CO, NO and hydrocarbons under variable air/fuel conditions [4]. Stabilization of the ceria surface area has also been identified as an important benefit. Various researchers have examined Ce–Zr oxides both with and without precious metal loading in model systems and on monoliths under simulated exhaust conditions [5–8].

One interesting aspect of these systems is understanding the mechanisms by which the oxide components and precious metals interact to bring about enhanced catalytic activity. It has already been reported that synergism between the precious metal and the oxide occurs in redox activity [2,9]. It has been reported that the presence of Rh can induce a very high efficiency of the Ce^{3+}/Ce^{4+} redox couple at temperatures as low as 440 K [9–11] or 294 K [12]. We report *in situ* XANES measurements which allow us to determine directly the degree of reduction of Rh-loaded and of Rh-free, high surface area, mixed Ce–Zr oxides during reduction conditions. We find that the Zr increases the extent of Ce reduction at temperatures above 600 K. We also find clear evidence that the presence of Rh catalyzes the reduction process at low temperatures at all Zr concentrations.

2. Experimental

Synthesis of oxides

Sol–gel syntheses of the mixed oxides were carried out using a modification of literature methods [13]. Mixtures of cerium(III) acetylacetonate (Aldrich) and zirconium(IV) butoxide (Aldrich) in absolute ethanol were refluxed for 3 h under Ar atmosphere. A mixture of ethanol and water (25 : 1) was then added and the solution refluxed overnight. Following reduction in volume by distilling off solvent, toluene was added to the remaining mixture which was transferred to an autoclave for hypercritical drying. The drying process involved pressurization under Ar and heating to 540 K followed by rapid depressurization to vent solvent. The resulting grayish fluffy solid was collected and calcined in air for 5 h at 775 K. The calcined products varied in color from cream (CeO_2) to bright yellow $(Ce_{0.5}Zr_{0.5})O_2$.

Portions of the oxides were impregnated with Rh. Measured aliquots of $Rh(NO_3)_3$ (Alfa-Aesar) dissolved in water were dosed onto the calcined oxide to give Rh loadings of 0.5 or 2% by weight. The solid was allowed to dry in air and then calcined at 775 K for 5 h.

The X-ray absorption measurements were recorded at the Ce L_{III} edge using beamline X-19a at the National Synchrotron Light Source. The monochromator incorporated a double Si crystal which was detuned (monitored by a 30% decrease in the incident X-ray flux) to remove third-order light. Reagent grade CeO_2 was used as a standard for Ce^{4+} and Ce(III) fluoride and Ce(III) acetylacetonate were used as standards for Ce^{3+} spectra. To make XANES targets, sol–gel samples were ground and mixed with alcohol or acetone to make a slurry, a few drops of which were deposited onto BN wafers and dried in air at room

temperature. The BN wafers were pressed from powder to thicknesses of 50–55 mg/cm^2 (roughly 50% transmission at the Ce edge). The treated wafer was captured on a stainless steel sled which was placed near the center of a quartz tube (56 cm long) which was positioned within a clam-shell tube furnace. Stainless steel fittings on the ends of the tube had rectangular windows covered with a polymer film to permit passage of the X-ray beam. A thermocouple inserted through a fitting at the downstream end was clamped to the sample sled. A gas manifold outside the X-ray hutch permitted control of gas flow through the tube. A mixture of 4% H_2 in He (Matheson) was used as a reductant, and zero air (Matheson) was used to reoxidize the sample.

3. Results

3.1. BET measurements

The surface areas of the powders were measured following calcining using a Quantachrome Autosorb apparatus. Calcining at 775 K had the effect of collapsing the surface areas from ∼450 to ∼100 m^2/g. Results of five-point BET measurements of the oxides are shown in table 1. No attempt was made to perform selective surface area measurements to obtain Rh dispersion. Such measurements are expected to be problematic due to strong adsorption capability of the ceria support [14].

3.2. X-ray diffraction

The sol–gel oxides were characterized by X-ray diffraction (XRD) using Cu K_α. For the hypercritically dried samples prior to calcining, the XRD patterns exhibited very broad features, but the major peaks were at the locations of a fluorite structure. Upon calcining to 775 K the lines sharpened. It was possible to assign all of the observed peaks to the fluorite structure for all samples indicating a single phase, solid solution. However, for all compositions the lines are broad enough that it is difficult to eliminate the possibility of a tetragonal distortion such as reported previously for oxides with $(Ce_{1-y}Zr_y)O_2$ with $y > 0.2$ [15,16]. Recent studies of $(Ce_{0.5}Zr_{0.5})O_2$ prepared by firing equimolar mixture of ZrO_2 and CeO_2 yielded lower surface area oxides and indicated only the cubic phase present, although unmixed CeO_2 was also present [17]. The measured peak positions in our 2θ scans and the resulting lattice constants, which decreased as the Zr content increased from $y = 0$ to 0.5 in the oxide, were in good agreement with previous data [3,15,18,19]. Calculations based upon the widths of the four lowest angle peaks yielded the mean crystallite sizes of the calcined oxides and the results are shown in table 1. The 2% $Rh/(Ce_{0.5}Zr_{0.5})O_2$ also showed only features due to the fluorite lattice. No features attributable to Rh metal, Rh oxide or Rh–Zr–Ce mixed oxide phases were visible, presumably due to low Rh loading and high dispersion. Therefore no information about Rh dispersion was obtained from XRD. The additional calcination of the 2% $Rh/(Ce_{0.5}Zr_{0.5})O_2$ led to a small increase in the mean particle sizes as determined by XRD and to a small decrease in the BET surface area.

Table 1
Surface areas and particle sizes as determined by BET and XRD measurements.

Oxide support	BET (m^2/g)		X-ray crystal size (nm)
	Rh-free[a]	2% Rh[b]	Rh-free
CeO_2	110	111	5.9
$(Ce_{0.9}Zr_{0.1})O_2$	94	95	4.7
$(Ce_{0.8}Zr_{0.2})O_2$	109	97	4.4
$(Ce_{0.7}Zr_{0.3})O_2$	187	118	4.0
$(Ce_{0.6}Zr_{0.4})O_2$	138	129	4.2
$(Ce_{0.5}Zr_{0.5})O_2$	154	147	4.0

[a] Rh-free samples calcined at 775 K for 5 h.
[b] Rh-loaded samples calcined 775 K an additional 5 h.

3.3. XANES spectra

The XANES spectra at the Ce L_{III} edge were obtained from each sample as the temperature was increased in steps. Typically, the sample was introduced to the reactor cell at temperatures of 300–350 K and He was flowed through the reactor cell long enough to purge most of the residual air. After this the first XANES spectrum was recorded followed by changing the gas flow to H_2/He and another measurement. Occasionally, the first measurement in He was omitted and the initial spectrum was recorded in H_2/He. The temperature was then increased and allowed to stabilize for another spectrum. Upon reaching the highest desired temperature the sample was cooled in reductant and further spectra recorded. In some cases, the sample was reoxidized in air and the changes followed by XANES.

A set of typical X-ray absorption spectra are shown in figure 1. The spectra clearly demonstrate the changes which occur in the Ce edge as a function of reducing temperature. The features observed in the Ce L_{III} absorption edge have been reported and assigned previously [11,20]. In particular, the peak labeled C, which is strong for fully oxidized CeO_2, has been assigned to absorption into the 5d level with no occupancy in the 4f level in either the initial or final state. Therefore this peak is only expected if Ce^{4+} is present. The peak labeled B_1 shows a clear splitting into B_1 and B_2 components for the reagent CeO_2, but this splitting was much less apparent in the sol–gel derived ceria catalysts. These features are associated with occupancy of the 4f level in the final state. Upon reducing the sample a new peak, labeled B_0, grows in at an energy slightly below the B_1 peak, and is associated with 4f occupancy in the initial state. This peak is therefore indicative of the presence of Ce^{3+} in the sample. In summary, reduction of the sample is associated with a growth of the B_0 peak and a decrease of the B_1 and C peaks. This trend is easily seen in the raw spectra.

Various methods were attempted to quantify the extent of the reduction. Curve fitting of the data in a manner such as described by El Fallah [11] was attempted but seemed to

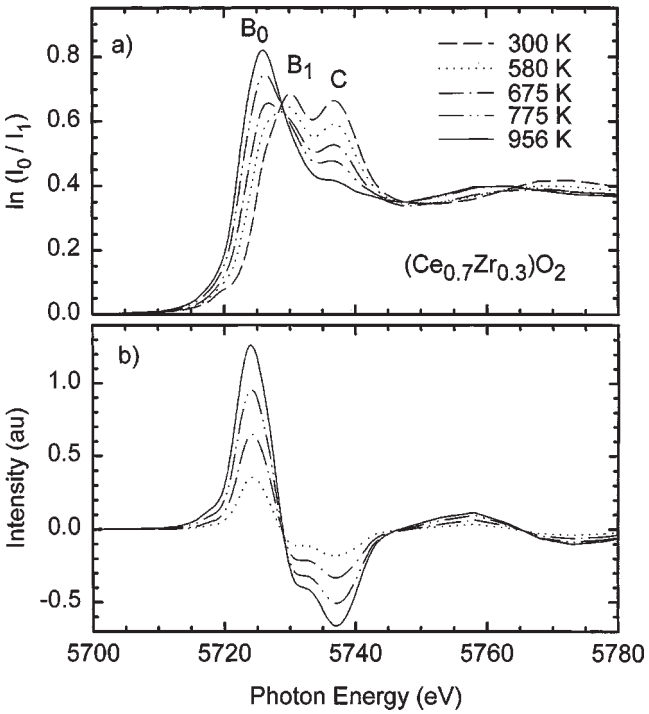

Figure 1. XANES spectra are shown in (a) for the $(Ce_{0.7}Zr_{0.3})O_2$ sample during reduction at various temperatures. A linear background has been subtracted from each spectrum. In (b), the difference spectra are shown which are obtained by normalization of all spectra to unity at 5830 eV followed by subtraction of the spectrum obtained at 300 K.

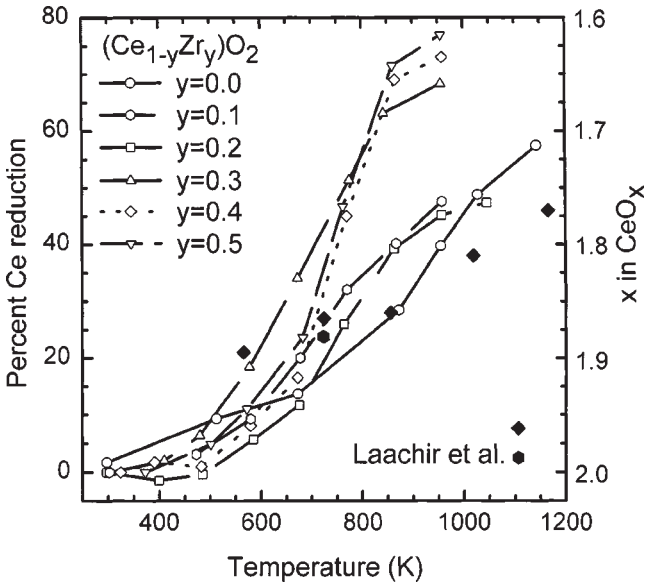

Figure 2. Percent reduction and corresponding x (in CeO_x) is shown versus temperature for different samples (open symbols). Reduction is determined from the Ce XANES using the difference procedure described in the text and using the lowest-temperature spectrum as reference. Previous results from Laachir et al. [21] for a high surface area CeO_2 using XPS and magnetic susceptibility are shown for comparison (filled symbols).

give ambiguous results due to uncertainty in the location of the continuum step edge. In addition, there was variation between the relative intensities of the step edge compared to the height of the C peak above it, making it difficult to correlate the C peak intensity directly with extent of reduction. This relative intensity variation was observed even when comparing all the fully oxidized samples, and was attributed to variation in sample thickness (both from sample to sample and across a single target).

To minimize these effects the following simple procedure was used to extract the degree of reduction. A linear background was subtracted from each absorption curve, expressed as $\ln(I_0/I_1)$. This method generally gave a nearly flat continuum edge above the peaks, as seen in figure 1. The background corrected spectra were then normalized at a point above the edge. On the assumption that the overall sample morphology and thickness variation across the target was preserved throughout the reductive cycle, the initial spectrum recorded at low temperature was used as a reference of the fully oxidized sample. This spectrum was subtracted from each spectrum subsequently obtained at higher temperatures. This procedure results in a series of difference curves such as shown in figure 1(b). The effect of reduction is clearly seen as a negatively increasing C peak and a positively increasing B_0 peak. Their difference was assumed to be proportional to the extent of reduction. This method makes use of the information contained in both the C and B peaks. It also minimizes complications due to variation relative to the step intensity. The normalization process makes the numbers transferable to other samples. Since all spectra in a given reduction set are compared only to the initial fully oxidized sample, variations in thickness homogeneity from sample to sample are not magnified.

A similar procedure was used to compare a spectrum from CeF_3 with that from either reagent grade CeO_2 or the sol–gel derived CeO_2. This yielded difference curves very similar to those obtained for the reduced samples. The $C - B_0$ value obtained for this reference should describe a sample fully reduced (to Ce^{3+}). This value was then used to normalize the values obtained from the other samples and determined their extent of reduction.

Resulting values are shown in figure 2 for various of the sol–gel derived oxides as a function of the Zr content. It is seen that with increasing Zr content, the extent of reduction achieved at a particular temperature increases, for temperatures above 600 K. By 900 K, the Zr-doped samples ($y > 0.3$) achieve an extent of reduction which is higher than that achieved by the undoped CeO_2 at any temperature up to 1200 K.

The effect of adding Rh to the sample is shown in figures 3 and 4. It is seen in these data that the presence of Rh greatly enhances the extent of reduction achieved at low temperatures. The enhancement is seen at temperatures as low as 400 K. The amount of enhancement depends upon the Zr content but it is seen even in the sample without Zr. Unfortunately, insufficient data were obtained at low temperature to clearly determine the onset temperature for this reduction or how it depends upon Zr content. Although the reduction is enhanced at low temperatures, the extent of reduction achieved at higher temperatures is not larger than is obtained for the Rh-free samples of the same composition,

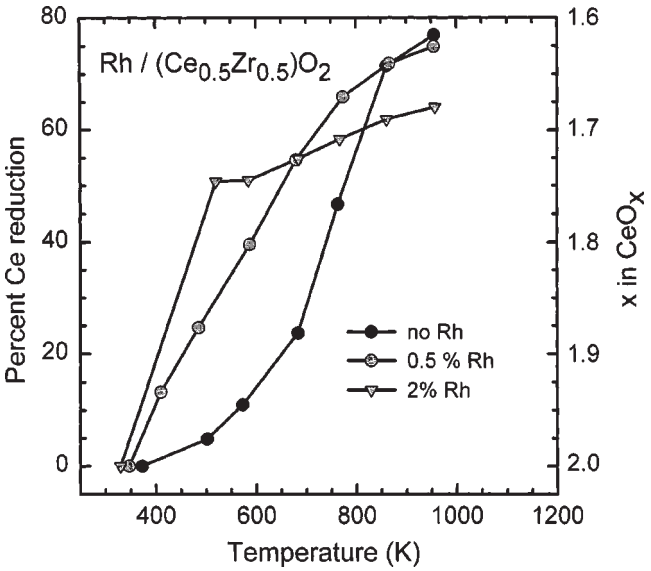

Figure 3. Percent reduction and corresponding x (in CeO_x) is shown versus reduction temperature for two different Rh loadings on $(Ce_{0.5}Zr_{0.5})O_2$.

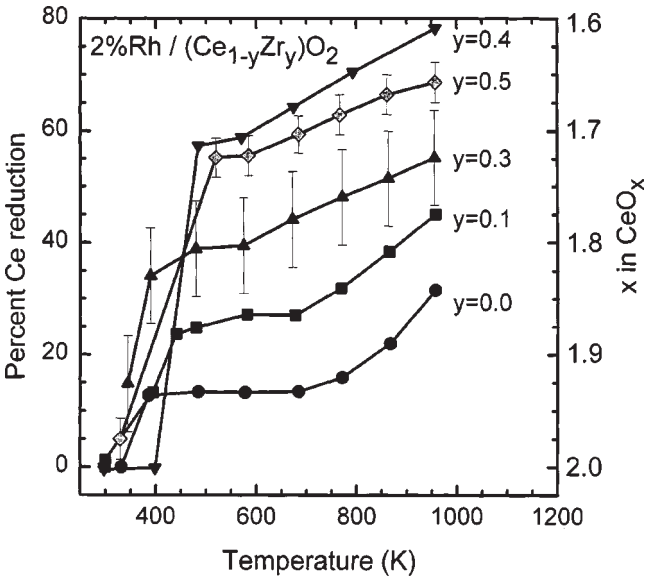

Figure 4. Percent reduction and corresponding x (in CeO_x) is shown versus reduction temperature for samples with 2% Rh on different mixed oxides, $(Ce_{1-y}Zr_y)O_2$. For the samples with $y = 0.3$ and $y = 0.5$, the degree of reduction and error bars were obtained from the average value obtained by referencing to various different oxidized samples.

except possibly for the $(Ce_{0.6}Zr_{0.4})O_2$ sample. This can be seen by comparing figures 2 and 4.

Since the reduction occurs rapidly at low temperatures for the Rh-loaded samples, there is the possibility that at the initial temperatures (300–350 K) samples in H_2/He may already be partly reduced. Because this initial spectrum provides a reference for all the higher-temperature data, partial reduction at the initial temperature would have the effect of depressing the apparent degree of reduction at higher temperatures. This was suspected for the two samples with $y = 0.3$ and 0.5 (figure 4) for which an initial spectrum in He was not obtained. To assess the extent of possible initial reduction, various other reference spectra were applied for these samples. Spectra obtained for other targets, chosen to be of similar thickness and Zr content and obtained under conditions where they would be fully oxidized, were subtracted from the data. The data shown in figure 4 for these two samples are average values obtained using various reference spectra. The error bars represent the standard deviation of this average and provide an estimate of the uncertainties due to the referencing procedures and to sample-to-sample variations.

4. Discussion

Reduction of ceria by hydrogen has been described as falling into two types, reduction associated with the reversible uptake of hydrogen and "irreversible" reduction associated with loss of water [14]. It has been shown that both processes lead to a change in the Ce oxidation state from Ce^{4+} to Ce^{3+} [12,14,21] and so XANES should be sensitive to either. However, from the current results it is not possible to determine the extent of water elimination.

The degree of reduction measured by XANES can be compared against previous results. In figure 2, the filled diamonds summarize results for reduction of CeO_2 [21]. Those measurements were based upon analysis of X-ray photoelectron spectroscopy (XPS) of a 115 m^2/g ceria sample following reduction in 1.0 MPa H_2 for 4 h at each temperature. The agreement validates that the XANES yields an accurate assessment of the degree of reduction. The XPS results yield a slightly higher degree of reduction below 800 K, possibly due to a difference in reduction times which in the present case were on the order of 10 min. Laachir et al. [21] reported magnetic susceptibility measurements which showed that at temperatures of 650–700 K the degree of reduction increases from about 23 to 31% when the reduction time is increased from 2 to 20 h, bracketing their XPS result of about 27% near this temperature.

Fornasiero et al. [9] have measured the degree of reduction by oxygen uptake for a sample of 0.5% Rh-loaded $(Ce_{0.5}Zr_{0.5})O_2$. They report that, for this sample reduced at 1273 K, the Ce^{3+} fraction is 58–64%, depending on the number of oxidation/reduction cycles carried out. For a sample reduced at 440 K for 2 h, they report 50% Ce^{3+}. These values agree well with the one-cycle reduction data shown in figure 4 for the 2% $Rh/(Ce_{0.5}Zr_{0.5})O_2$ where above 450 K the Ce^{3+} fraction varies from 55 to 65%.

The rate of reoxidation was faster than the rate of reduction, since reoxidation occurred rapidly at low temperatures. In one experiment, the $(Ce_{0.5}Zr_{0.5})O_2$ sample was measured to be about 75% reduced following treatment in H_2 at 975 K. It was then cooled in H_2/He to $<$410 K and verified to still be highly reduced. The sample was further cooled to 300 K and then air was introduced. XANES then indicated that the sample was fully oxidized. Rapid reoxidation could also be inferred from the difficulty of cooling samples in H_2/He without partial reoxidation. A liquid

nitrogen-cooled trap containing zeolite was used on the inlet line to trap water and to decrease the impurity partial pressure of O_2. In spite of these additional precautions, the reduced samples, especially the Zr-free ceria, were very difficult to cool without reoxidation. Evidently, the ratio of oxidant to reductant level must be very low to prevent rapid reoxidation.

The ease of reoxidation has been noted previously [11, 21]. Linear uptake of oxygen at room temperature was measured by magnetic susceptibility for a reduced CeO_2 [21]. Reoxidation was found to be complete for two samples with widely different surface areas indicating that the reoxidation process does not depend upon the texture. In a XANES study, reoxidation of CeO_2 at 673 K by air was complete and the rate was too fast to be measured [11]. These and the present results might suggest that oxygen migration is not the limiting step in the slower reduction process. Thermodynamically, however, the reoxidation of Ce_2O_3 by O_2 or water is so strongly favorable that rapid reoxidation does not necessarily eliminate the possibility that oxygen diffusion is rate limiting. Direct evidence that oxygen diffusion from the bulk to the surface does not control the kinetics of oxygen release has been reached previously from studies of CO oxidation rates by CeO_2 and by $(Ce_{0.75}Zr_{0.25})O_2$ [22].

An important result is that Rh has the effect of bringing about reduction at low temperature. When the $(Ce_{0.5}Zr_{0.5})O_2$ sample has 2% Rh present it is extensively reduced already at 473 K (figure 4). Enhanced reduction was seen by 473 K for all of the oxides, but the extent of the low-temperature reduction increases with Zr concentration. Apparently, the Rh is catalyzing the reduction of the oxide substrate, so that reduction occurs at a much lower temperature than in its absence. Fornasiero et al. also noted high efficiency of reduction at temperatures as low as 440 K from temperature-programmed reduction (TPR) of 0.5% $Rh/(Ce_{0.5}Zr_{0.5})O_2$ [9] compared to a Rh-free sample, and the effect has been seen previously by XANES for Rh/CeO_2 [11]. The low-temperature state seen in TPR is clearly not due only to reduction of Rh but is due also to reduction of the oxide substrate [8,9].

Although the Rh speeds up the rate of reduction, the ultimate degree of reduction achieved at higher temperatures does not increase over that for the Rh-free samples. As seen in figure 3 for the sample with 2% Rh, further heating above 475 K only increases the degree of reduction from about 55 to 65%. The degree of reduction achieved at 973 K was not enhanced by the presence of Rh for this sample, nor for those of any other Zr content. Evidently, whatever catalytic effect the Rh has, it does not lead to complete reduction or to enhancement of the high-temperature reduction processes.

What are the causes of the enhanced reduction induced by Rh? Rh is readily reduced under low-temperature conditions, as indicated by TPR measurements, and it has been demonstrated to produce spillover hydrogen onto a ceria support [8,12]. A ceria sample showed uptake of hydrogen and Ce reduction at 295 K when Rh was present, while a similar sample without Rh showed negligible hydrogen uptake at this temperature [12]. Production of a mobile reactant explains why a small amount of Rh could affect the entire support. Another possibility is that Rh may enhance dehydroxylation of the ceria. Gravimetric measurements [21,23] and temperature-programmed desorption measurements [14] indicate that elimination of water does not occur until above 525 K. It may be possible that Rh serves to catalyze desorption of H_2O from the oxide surface by reaction between a substrate oxygen or hydroxyl and hydrogen adsorbed on Rh. Such reactions between species adsorbed on Rh with oxygen from the reduced support have been observed previously [24]. Furthermore, contact between the Rh and the reduced support can lead to interesting variations in the catalytic properties of the Rh. Adsorption and dissociation of NO and CO on Rh-loaded CeO_2 single crystals are observed to depend upon the degree of reduction of the support [25,26].

The present XANES study confirms the enhanced reducibility of ceria caused by Zr addition, previously inferred from CO oxidation measurements [3] and from TPR results [17]. $(Ce_{0.5}Zr_{0.5})O_2$ which has undergone a few redox cycles shows TPR peaks in the range of 700 and 850 K compared to similarly treated CeO_2 which does not show onset of reduction until above 900 K [17]. The XANES results shown in figure 2 are qualitatively in agreement with this trend. Little or no difference in reduction is observed on any sample below 500 K and no effect of Zr is observed until 600 K or higher. Above 600 K, Zr enhances the extent of reduction for all Zr additions, although the effect is most pronounced for $y \geqslant 0.3$. Interpretation of the two or three peaks in TPR data suggests that surface reduction precedes bulk reduction [17]. The present one-cycle XANES data do not indicate a plateau or feature that distinguishes a difference between surface and bulk reduction. This may be in part due to the high dispersion of these oxides.

The effect of the Zr addition is most pronounced in samples which contain Rh. For the Rh-containing samples, the Zr systematically enhances the low-temperature reducibility, as seen in figure 4. Together, the Rh and Zr additions create a catalyst in which the extent of substrate reduction is nearly constant over a wide temperature range and the higher the Zr content the higher the extent of reduction. It may be expected that this synergism could lead to a catalyst with high oxygen storage capability which operates consistently over a wide temperature range.

Based upon concepts and conclusions described above, all of the present results and the apparent interactions between ceria, zirconia and Rh can now be interpreted as follows. The Rh and the Zr additions enhance different steps in the reduction. Rh plays a role in enhancing the reversible uptake of hydrogen, leading to low-temperature reduction. Temperatures in the range of 350–450 K are sufficient to reduce the Rh [8], and once this has occurred rapid spillover of hydrogen from Rh onto the ceria is possible. Reduction of Rh followed by H uptake and spillover onto the oxide is responsible for the step increase in per-

cent reduction observed in figure 4 between 300 and 450 K. On the Zr-free ceria, the extent of low-temperature reduction is 10–20%. Based upon the surface area, this may correspond roughly to complete coverage of the ceria surface by hydroxyls [12]. Further reduction does not occur below about 800 K, above which point water removal has occurred [14,21,23] and onset of bulk reduction begins [21].

Zr plays a role in enhancing the migration of oxygen between the bulk and surface. This may occur due to alteration in the lattice constant or similar structural alteration of the defective, reduced oxide as suggested previously [17, 27]. The effect depends upon the concentration of Zr, as seen in figure 2, so greater Zr concentration gives oxygen transport to a larger fraction of the Ce ions. The enhancement may occur over a wide temperature range, but is not evident at temperatures below about 600 K in the Rh-free samples. This is because the slow uptake of hydrogen limits the reduction below 600 K for the Rh-free oxides, a problem for ceria which is not helped by the addition of Zr (figure 2). However, the addition of Rh facilitates hydrogen uptake and resulting hydroxyl formation. Since the extent of reduction observed at low temperature on the Zr-free Rh/CeO_2 corresponds to complete surface reduction, then the additional reduction achieved by Zr addition (figure 4) indicates bulk reduction at 500 K or possibly lower. Therefore, it can be inferred from figure 4 that the Rh may also catalyze elimination of water which is required for bulk reduction. A dual role of Rh and the contributing effect of Zr explains the very high reduction achieved at low temperatures for $Rh/(Ce_{1-y}Zr_y)O_2$ and $y \geqslant 0.3$. This model suggests that efficient reduction of the $(Ce_{1-y}Zr_y)O_2$ might occur at temperatures lower than 400 K if reduced Rh were present, a condition that was not achieved in these experiments.

This study demonstrates that XANES can be used to reliably estimate the extent of reduction of the supports in these catalysts. Further, it can allow dynamic measurements without interrupting reaction conditions or destroying the current reduction state as is required in TPO/TPR measurements. The measurement is specific to the Ce^{3+}/Ce^{4+} ratio and is unaffected by presence of chemisorbates or evolution of desorption products which may interfere with TPR/TPO measurements. Although there are difficulties with maintaining optimal conditions for both flow reactor kinetic studies and X-ray transmission or fluorescence studies, it is in principle possible to monitor the extent of reduction in ceria-based catalysts while simultaneously carrying out measurements of product yields and selectivities. This *in situ* capability may serve to probe further the links between catalytic reactivity and substrate redox properties which are believed to be so important in three-way conversion catalysts.

Acknowledgement

Research sponsored by the Division of Chemical Sciences, Office of Basic Energy Sciences, US Department of Energy, under contract DE-AC05-96OR22464 with Oak Ridge National Laboratory, managed by Lockheed Martin Energy Research Corp. GNG acknowledges support of the Great Lakes College Association/Associated Colleges of the Midwest. The National Synchrotron Light Source at Brookhaven National Laboratory is supported by the Division of Chemical Sciences and Division of Material Sciences of the US Department of Energy under contract DE-AC02-76CH00016.

References

[1] H.C. Yao and Y.F.Y. Yao, J. Catal. 86 (1984) 254.
[2] J.G Nunan, H.J. Robota, M.J. Cohn and S.A. Bradley, J. Catal. 133 (1992) 309.
[3] M. Ozawa, M. Kimura and A. Isogai, J. Alloys Comp. 193 (1993) 73.
[4] T. Murota, T. Hasegawa, S. Aozasa, H. Matsui and M. Motoyama J. Alloys Comp. 193 (1993) 298.
[5] J.G. Nunan, W.B. Williamson and H.J. Robota, SAE paper 960798 (1996).
[6] H. Permana, D.N. Belton, K.M. Rahmoeller, S.J. Schmieg, C.E. Hori, K.Y.S. Ng and A. Brenner, SAE paper 970462 (1997).
[7] P. Fornasiero, G. Balducci, J. Kašpar, S. Meriani, R. Di Monte and M. Graziani, Catal. Today 29 (1996) 47.
[8] P. Fornasiero, R. Di Monte, G.R. Rao, J. Kašpar, S. Meriani, A. Trovarelli and M. Graziani, J. Catal. 151 (1995) 168.
[9] P. Fornasiero, J. Kašpar and M. Graziani, J. Catal. 167 (1997) 576.
[10] A.J. Soria, A. Martinez-Arias and J.C. Conesa, Vacuum 43 (1992) 437.
[11] J. El Fallah, S. Boujana, H. Dexpert, A. Kiennemann, J. Majerus, O. Touret, F. Villain and F. Le Normand, J. Phys. Chem. 98 (1994) 5522.
[12] S. Bernal, J.J. Calvino, G.A. Cifredo, J.M. Rodriguez-Izquierdo, V. Perrichon and A. Laachir, J. Catal. 137 (1992) 1.
[13] S. Meriani and G. Soraru, in: *Ceramic Powders*, Materials Science Monographs, Vol. 16, ed. P. Vincenzini (Elsevier, Amsterdam, 1983) p. 547.
[14] S. Bernal, J.J. Calvino, G.A. Cifredo, J.M. Gatica, J.A.P. Omeil and J.M. Pintado, J. Chem. Soc. Faraday Trans. 89 (1993) 3499.
[15] S. Meriani and G. Spinola, Powder Diffraction 2 (1987) 255.
[16] M. Yashima, H. Arashi, M. Kakihana and M. Yoshimura, J. Am. Ceram. Soc. 77 (1994) 1067.
[17] P. Fornasiero, G. Balducci, R. Di Monte, J. Kašpar, V. Sergo, G. Gubitosa, A. Ferrero and M. Graziani, J. Catal. 164 (1996) 173.
[18] D. Dragoo, Natl. Bur. Stand. Monograph 25(20) (1983) 38.
[19] G. Passerini, Chim. Ital. 60 (1930) 766.
[20] D.D. Beck, T.W. Capehart and R.W. Hoffman, Chem. Phys. Lett. 159 (1989) 207.
[21] A. Laachir, V. Perrichon, A. Badri, J. Lamotte, E. Catherine, J.C. Lavalley, J. El Fallah, L. Hilaire, F. LeNormande, E. Quemere, N.S. Sauvion and O. Touret, J. Chem. Soc. Faraday Trans. 87 (1991) 1601.
[22] C.E. Hori, H. Permana, K.Y.S. Ng, A. Brenner, K.M. Rahmoeller, S.J. Schmieg and D.N. Belton, Abstracts of 15th Meeting of the North American Catalysis Society, May 18–22, 1997.
[23] J.L.G. Fierro, J. Soria, J. Sanz and J.M. Rojo, J. Solid State Chem. 66 (1987) 154.
[24] T. Bunluesin, E.S. Putna and R.J. Gorte, Catal. Lett. 41 (1996) 1.
[25] S.H. Overbury, D.R. Huntley, D.R. Mullins, K.S. Ailey and P.V. Radulovic, J. Vac. Sci. Technol. 15 (1997) 1647.
[26] J. Stubenrauch and J.M. Vohs, J. Catal. 159 (1996) 50.
[27] G. Vlaic, P. Fornasiero, S. Geremia, J. Kašpar and M. Graziani, J. Catal. 168 (1997) 386.